J Electroceram (2010) 25:45–55
DOI 10.1007/s10832-009-9587-6

# Modal validation of a cantilever-plate bimorph actuator illustrating sensitivity to 3D characterisation

**Matthew J. Oldfield · Mark A. Atherton · Ron A. Bates · Mark A. Perry · Henry P. Wynn**

Received: 24 July 2008 / Accepted: 29 July 2009 / Published online: 13 August 2009


**Abstract** A dynamic finite element (FE) model of a small piezoelectric plate actuator with cantilever boundary conditions is validated experimentally using operating modes, as the scale of the device prevents conventional modal excitation. A general methodology is presented for assembly of 3D modal response of the plate surface from single-point laser vibrometer data, which is an economical alternative to the automated process provided by scanning vibrometers. 1D blocked force and 2D beam assumptions prove insufficient for validation due to modes both in the length and width of the device in operation. The model is validated in the audible frequency range encompassing 12 experimental operating modes. It is shown that when conducting validation using operating modes, the experimental results, simulated frequency response and FE eigenmodes must all be compared. Discrepancies between FE and experiment are identified and attributed to manufacturing imperfections above modelling errors.

**Keywords** Bimorph · Vibration measurement · Finite element methods · Cantilever plate · Experimental validation

M. J. Oldfield (✉) · M. A. Atherton
School of Engineering and Design, Brunel University, Uxbridge UB8 3PH, UK
e-mail: matthew.oldfield@brunel.ac.uk

M. A. Atherton
e-mail: mark.atherton@brunel.ac.uk

R. A. Bates · M. A. Perry · H. P. Wynn
Department of Statistics, London School of Economics, London WC2A 2AE, UK

R. A. Bates
e-mail: r.bates@lse.ac.uk

H. P. Wynn
e-mail: h.wynn@lse.ac.uk

## 1 Introduction

There is a scarcity of literature addressing modal validation of finite element (FE) models of devices too small for well-established experimental techniques and too complex to be validated against 2D structural assumptions. In this paper, a method is demonstrated for the validation of a multi-modal piezoelectric actuator over its operating frequency range. The method is configured to provide modal actuation and results that fully characterise behaviour and provide sufficient data to accept or reject the model as validated. Using operating conditions and pointwise measurement, the reader is shown a methodology and results for fully establishing the operating modal response. Comprehensive 3D analysis is required for this cantilever-plate-based device before validation is established.

Piezoelectric materials are increasingly used as sensors and actuators due to their efficient coupling of energy in the electrical and mechanical domains. As such they have been used in a cantilever configuration as actuators [1, 2], control devices [3, 4] and as modally controlled sensors [5] incorporating micro-scale [6] and macro-scale components [7]. For the actuator presented here it is economical to investigate changes in response through numerical modelling prior to physical prototyping. However, optimization of performance through numerical parameter adjustment can only be implemented once the model has been fully validated dynamically. Highly modal microscale devices are too small and operate at frequency ranges unsupported by conventional excitation devices. This prevents application of conventional modal analysis techniques and must be overcome. Discrepancies must be identified and either used to modify the FE model or rationalized as independent of the fidelity of the model.

Among analytical methods used to model the dynamic behavior of piezoelectric materials and devices, Tiersten's work [8] is one of the earliest applied to piezoelectric plates. Chen, Xu and Ding [9] consider a 3D state-space formulation for simply supported piezoelectric plates and compare this with a 2D approach. An exact solution in 3D for the eigenmodes of rectangular simply-supported piezoelectric plates is presented in [10] drawing attention to the large amount of electromechanical coupling that can exist. Benjeddou and Deü [11] have developed a method for analyzing the out-of-plane modes as well as the thickness modes of a piezoelectric sandwich plate. These studies reveal much about piezoelectric materials and their behaviour. However the structures and boundary conditions in many applications, including the device investigated here, are more complex and must be characterised before simplification. Analytical approaches to identifying the modes of plates subjected to a variety of boundary conditions have been presented by Gorman [12] and Leisa [13]. Blevins [14] approximates modal frequencies and profiles to those derived using individual beams along the two axes in the plane of the plate. Friswell [15] notes the absence of an exact theoretical solution for the modes of a cantilever plate and identifies FE as an appropriate modelling tool for this purpose.

An early example of FE that takes into account electro-mechanical interactions is provided by Allik and Hughes [16]. In [17] FE models are refined in a process to optimize performance characteristics for a sensitivity analysis. Optimisation is also performed through FE for a single mode of vibration in [18] but without demonstration of a validation process. In [19] FE optimisation and validation of a bimorph actuator is based on frequency response of just a single mode. A FE model of an omnidirectional piezo-actuator is shown in [20] with 3D validation of a single mode despite simulation of multiple resonances. Multiphysics-type FE software is able to address many of the issues raised in [21] such as dynamic modeling using modal coordinates and efficiently linking multi-energy domains with both conservative and dissipative components. An FE model of the piezoelectric device is constructed here but analyses show discrepancies with reduced-dimension experimental observations.

In [22] a macro-scale piezoelectric device is measured modally using conventional hammer testing. A limited number of modes in 3D are identified in [23] and the significance of the excitation method used in revealing certain modes is illustrated. Ewins [24] presents many of the useful techniques used in modal analysis and dynamic validation. 3D Microscale modal identification has been undertaken successfully for a limited number of modes by Schnitzer [25] and Chu et al. [26] but without reference to a numerical model of any kind. In [27] and [28] successful microscale modal analysis is carried out on structures where the range of modes of interest are established in 2D. Lai and Fang [29] demonstrate global excitation on a 2D microscale device provided by an acoustic hammer. Ozdoganlar, Hansche and Carne [30] outline more fully a methodology for the modal analysis of microscale cantilever beams. The number of modes used to identify beam loss factors are insufficient for modes across the beam's width to be displayed.

Where 3D measurements have been made no comparison exists with a corresponding representative model. Alternatively where models are developed, the devices and significant operating modes require no measurements beyond 2D. In the device validated here the operating frequency range includes modality across the entire plate surface and introduces additional geometric considerations. Experimental hammer tests and data collection using device-mounted accelerometers are not suitable at the bimorph's scale. MEMS devices often have resonant frequencies of interest extending beyond the capabilities of conventional shakers. In [31] 3D microscale analysis is successfully implemented for limited modes using piezoelectric base excitation. Here calibrated excitation using the device itself is demonstrated, eliminating the need for specialist equipment capable of high frequency actuation.

There are many complicating factors for an analytical prediction of the modes of a piezoelectric plate actuator: The plate is multilayered, coupling exists between the PZT material, applied voltage and mechanical behavior [32] and the influence of non-ideal boundary conditions is undetermined. The bimorph's scale makes it susceptible to production inaccuracies that would be within acceptable tolerances in a macro-scale device. Identifying and characterising these inaccuracies is critical to achieving validation, and illustrates the limitations of relying on FE or experimental results alone.

The work presented here develops an experimental methodology based on approaches in [24] and [30] necessary for 3D microscale modal analysis. This method is required for validation of a 3D FE model following results indicating significant modes in both the plate's length and width coupled with discrepancies between the model and 1D and 2D experimental results. Results are obtained without recourse to scanning vibrometer technology.

## 2 Device under investigation

The device under investigation, known as a Single Layer Distributed Mode Actuator (SLDMA) (Fig. 1), is used to create an audible response in an acoustic panel—approximated to between 20 Hz and 20 kHz—from an electric potential input.

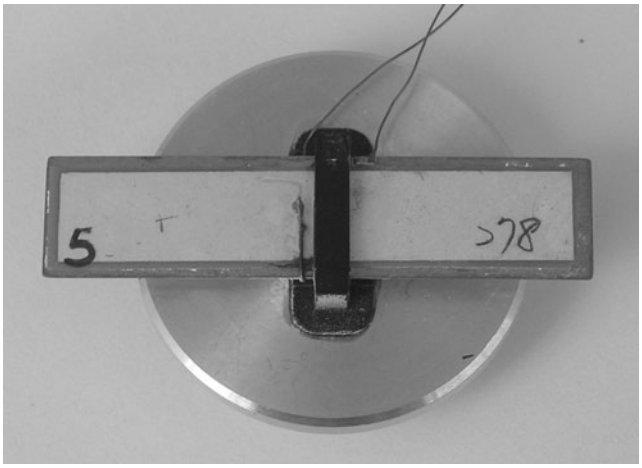


**Fig. 1** The SLDMA device attached to an aluminum base for testing. Viewed from an out-of-plane direction

An active layer is attached on each side of a brass shim using an epoxy adhesive. The active layers consist of a layer of PZT5H material between two silver electrodes. This 9-layer 'active plate' is held in a stub made from ABS plastic. The stub is attached by its base to transfer the vibrations of the plate to the acoustic panel. The depths of each layer are given in Table 1.

The brass shim has a nominal length and breadth of 34 mm and 8 mm respectively. The plate, consisting of active layers, epoxy and brass shim, is positioned by hand in the stub at a nominal offset of 1 mm from its midpoint.

Figure 2 shows the applied voltage conditions at the electrodes. By poling the PZT5H normal to the plane of the plate one PZT5H layer expands while the other contracts causing bending of the plate. Dynamic bending of the plate results in an inertial force that is transferred through the base of the stub.

A 3D FE model that incorporates the structural dynamics and electro-mechanical interactions of the device is presented. The model is built and run using the commercially available Comsol Multiphysics software. Eighteen eigenmodes are extracted in the audible range and frequency response simulations under operating conditions are performed. The need to represent the SLDMA in 3D is illustrated by significant deformations in the dimension of the plate's width that cannot be represented adequately using a 2D beam assumption.

**Table 1** Components making up the plate of the SLDMA.

| Layers in sequence | Nominal depth (μm) |
|---|---|
| Silver electrode | 5 |
| PZT-5H | 100 |
| Silver electrode | 5 |
| Epoxy adhesive | 12 |
| Brass shim | 100 |
| Epoxy adhesive | 12 |
| Silver electrode | 5 |
| PZT-5H | 100 |
| Silver electrode | 5 |

Correlation is achieved between FE and experimental frequency response tests using both blocked force and velocity as measured outputs. Neither 1D blocked force measurements nor a 2D beam assumption can explain the discrepancies existing between the model and experiment. A 3D surface profile alone is capable of identifying torsional modes in the experimental SLDMA. These torsional modes are caused by the sensitivity of the SLDMA to production errors and must be separated from the experimental response in order to validate the FE model.

## 3 Experimental configuration and parameters

An experiment was set up to measure the frequency response of five SLDMA devices. In operation the stub is assumed to be rigidly fixed to a stationary surface.

For all experiments the SLDMA is attached to an aluminum mount using cyanocrylate adhesive with the mount in turn tightly screwed into a force transducer (Endevco Model 2312). To isolate the signal from the SLDMA the force transducer is rigidly fixed onto a relatively massive block (Fig. 3). This configuration allows a frequency response of blocked force to be collected for the validation process. In a blocked force configuration the stub is provisionally assumed to provide a cantilever constraint with negligible gradient and deflection at the stub.

A swept sine input voltage from 20 Hz to 22.4 kHz is applied to a pair of the SLDMA electrodes in a configuration shown in Fig. 2. The remaining pair of electrodes are grounded.

An overview of the experimental setup is shown in Fig. 4. To coordinate the input and output signals to the SLDMA and from the force transducer a ClioQC system (Model 4 power amplifier & switching box with PC controlled signal conditioner) is used. Although the frequency response of the SLDMA is not flat with regard to frequency the input is automatically controlled via the ClioQC equipment to generate a voltage of 1 V root-mean-squared (RMS), with negligible variation at all frequencies. This is monitored using an oscilloscope (Kenwood 20 MHz Oscilloscope).

The input signal is taken to be the voltage supplied to the electrodes. This reflects the approach used in [30] and also the difficulty of maintaining a constant input force in a device that is modal in the frequency range investigated.

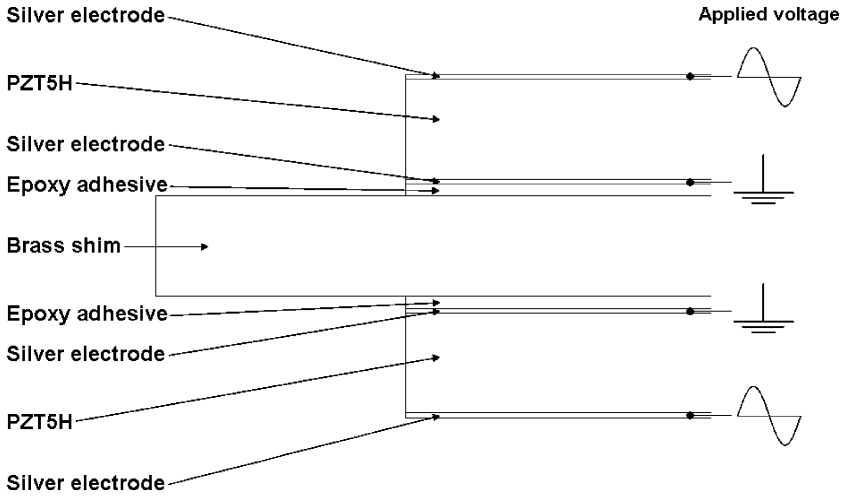


**Fig. 2** Cross section of the SLDMA showing layering of materials and applied electrical boundary conditions

Phase shifts are calculated in the ClioQC system by comparing the input signal and the blocked force output of the SLDMA. Output from the force transducer is converted into a measured voltage after passing through a signal conditioner (ENDEVCO Model I33). The resolution of the frequency response measurement is 537 logarithmically spaced readings.

In later experiments velocity measurements are required. A non-contact laser vibrometer (Polytec CLV700) replacing the signal from the force transducer shown in Figs. 3 & 4. The output from the vibrometer is routed through an additional integral signal conditioner.

## 4 Experimental blocked force frequency response

Figure 5 shows the frequency response from a collection of five SLDMAs. Over the tested range there is a variation in resonant frequencies but the overall shape of the frequency response shows good consistency. This indicates that discrepancies are due to small variations in material properties and physical construction.

The overall response can be characterised as having a resonance in the following frequency ranges: 0.5–0.6 kHz, 3–4 kHz, 10–11 kHz and 13–14 kHz. For SLDMA-1 and SLDMA-5 these first two resonances display a pair of modes instead of a single peak because they are assumed to behave as two cantilevered plates clamped at the stub. Increasing offset would increase the difference between resonant frequencies of the pair of assumed cantilever plates.

With only 1D blocked force measurements it is not possible to state whether modes are paired or approximate to cantilever plate vibrations. The blocked force measurements can only present a portion of the information required to fully characterise the SLDMAs for validation. With many modes in the relevant frequency range traditional 1D impedance measurements offer similar limitations.

## 5 Formulation of the FE SLDMA model

The FE SLDMA model (Fig. 6) uses dimensions of the five SLDMAs tested experimentally. Geometric parameters are mean values from measurement of the set of devices. As the SLDMA plate is only available fully assembled the thickness of each layer is assumed to be that nominally specified by the manufacturer.

The material parameters listed in Table 2 are specified by the manufacturer in the case of the ABS stub, or

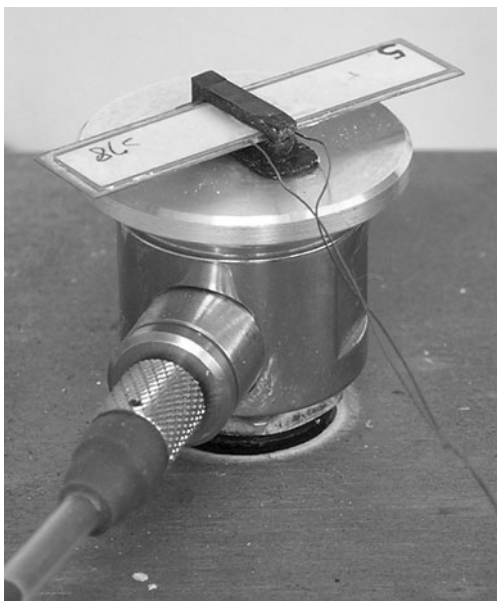

**Fig. 3** The SLDMA mounted on an aluminum plate that is screwed rigidly into a force transducer

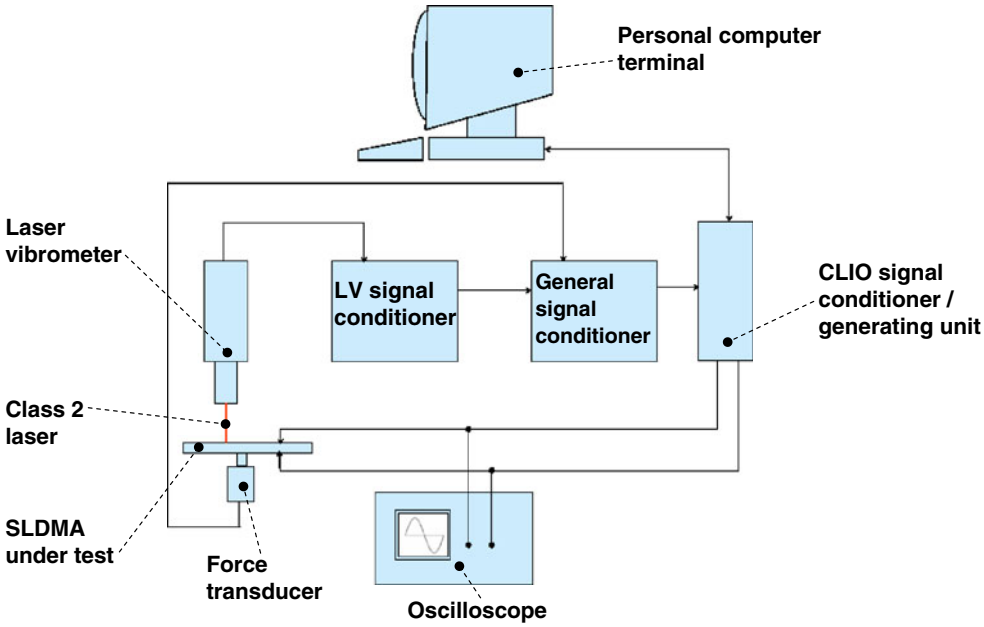


**Fig. 4** Schematic of the experimental setup illustrating the configurations for both the force transducer and laser vibrometer

estimated from a range of values given in [33]. PZT5H material parameters are specified in the stress-charge form shown below [34] with default parameters for PZT5H specified in Comsol Multiphysics.

$$T = c^E S - e_t E \tag{1}$$

$$D = eS + \varepsilon^S E \tag{2}$$

Where $T$=stress N/m$^2$, $c^E$=Elastic stiffness constant N/m$^2$, $S$=Strain, $e_t$=Piezoelectric stress coefficient C/m$^2$, $E$=Electric field V/m, $D$=Electric displacement C/m$^2$, $\varepsilon^S$=Electric permittivity F/m.

A mesh resolution is used that gives convergent results and satisfactory aspect ratios in the epoxy layer. The thinnest silver layers are omitted from the model to ease processing requirements and to compensate for the loss of material the PZT layers are thickened by 10 microns. Damping in the SLDMA is assumed to result primarily from the epoxy layers and due to their volume is considered negligible. It is removed from the model to ease computational cost and increase definition of resonant response. In lightly damped structures, only small changes to the resonant frequencies of the model result. Acknowledging that mode shapes are less sensitive to changes in material parameters than modal frequencies [5], the essential character of the model remains acceptably maintained.

In order to match the experimental conditions a voltage of 1 V RMS is applied to the outer faces of the PZT layers with the inner faces grounded. An Encastré constraint is applied to the bottom surface of the stub element to replicate the blocked force configuration.

## 6 Simulated blocked force response results

The FE blocked force frequency response allows initial comparison with the experimental data. Frequency was varied from 200 Hz to 20 kHz to cover the significant range of the experimental results. Results from the FE test are shown in Fig. 7.

Key features associated with the experimental blocked force frequency response are visible in the simulation plot. There appear to be two clearly defined pairs of peaks below 5 kHz with another pair close to 10 kHz. Resonances at higher frequencies, like those in the experiments, are closely bunched making it uncertain which higher frequency peaks form a pair.

The variability between the test samples (shown in Fig. 5) would make an exact match an anomaly and result in failure to match remaining experimental samples. More than general agreement is unlikely as the material parameters used in the FE model are approximations and can vary significantly between samples under test.

A similar envelope, but existing at higher frequencies, suggests that the FE model is generally stiffer than its experimental counterpart. This may be due to the inaccuracy of the material stiffness parameters used in the model. Joints are also a common cause of loss of stiffness in experiments and in the SLDMA there is potential for this between the stub and the plate.

Figure 7 demonstrates that making a reliable comparison between experimental and FE results is impossible, and although the envelopes of the frequency response show some correlation the resonant frequencies do not agree. The blocked force frequency responses provide an initial indication that the FE model can offer agreement

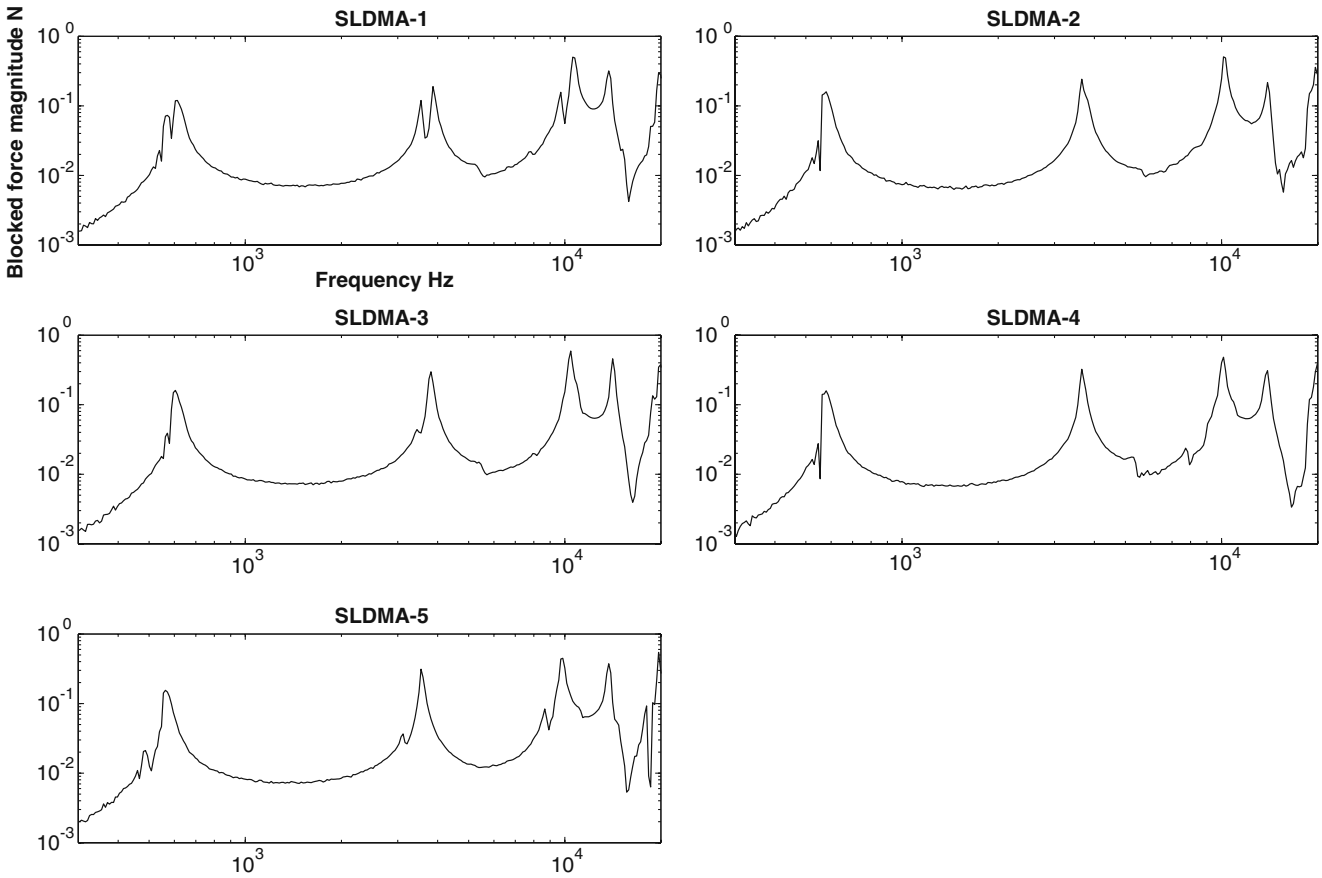


**Fig. 5** Experimental blocked force magnitude frequency response for the sample of 5 SLDMAs. The variability between devices is superimposed on an underlying consistency in frequency response characteristic

with the physical device under operating conditions. 1D results are not sufficient to reveal the nature of SLDMA behaviour and hence to allow validation.

## 7 FE eigenmode analysis

Despite variability between physical samples consistent trends have been identified with the FE response. Further information is required to correlate the FE model with experimental findings.

An FE eigenmode analysis is vital to understanding the character and sequence of operating modes. The eigenmode analysis presented here efficiently confirms that the SLDMA actuator behaves like a pair of cantilevered plates. This can be calculated two orders of magnitude quicker than a FE frequency response over the same frequency range.

Figure 8 shows the eigenmodes up to 20 kHz for the SLDMA model. There are 18 eigenmodes, considerably more than the number of resonant peaks of either the experimental or FE blocked force response.

The eigenmode analysis confirms pairing of plate modes on each side of the stub. The analysis also shows resonant frequencies in the FE model corresponding directly to eigenmodes with bending deflections. Torsional characteristics are present after only two preceding eigenmodes. The analysis also shows that above 18 kHz deformation across the width of the plate becomes significant. Consequently the 2D

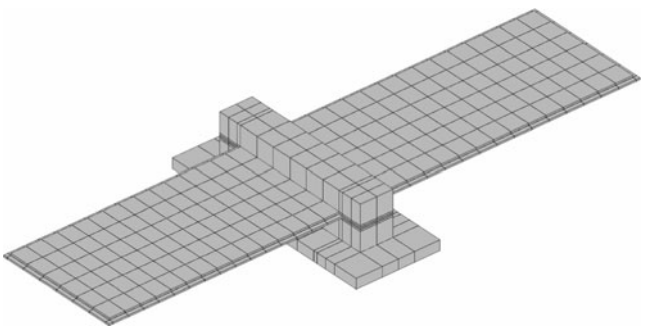

**Fig. 6** FE model constructed using mean sample measurements and with a 1 mm stub offset. The mesh is refined to give an acceptably converged solution

**Table 2** Material parameters used for the FE model of the SLDMA.

| Material | Density kg/m$^3$ | Young's modulus N/m$^2$ | Poisson's ratio |
|---|---|---|---|
| Brass | 8450 | $140\times10^9$ | 0.3 |
| Epoxy | 1200 | $3.8\times10^9$ | 0.3 |
| ABS | 1600 | $2.1\times10^9$ | 0.3 |
| PZT5H | 7500 | – | – |

modelling and results of [28], [22], [23] and [30] using a beam assumption would not be sufficient to characterise the SLDMA in its operating frequency range.

The in-plane eigenmodes (4350 Hz and 11390 Hz) will not be excited in operation as the PZT5H patches only actuate out of plane bending motion. Gorman [35] indicates that while torsional modes may be theoretically possible they will not be excited without a bias caused by a lack of symmetry under operating conditions. In some instances this is referred to as zero 'coupling' between the relevant eigenmodes and boundary conditions. However in operation this is not the same as zero output at the particular frequency. There will still be a response attributable to the small residual effects of the modes that are actuated. This 'coupling' should also not be confused with the critical electromechanical coupling in a bimorph described in [32].

In the idealized FE model symmetry is adhered to, but it cannot be guaranteed in the physical SLDMA.

Should torsional modes be excited the net simulated and experimental blocked force would be negligible. Over one half of the stub there will be a positive force and on the other half this will be negative. The net transfer of inertia is very small so the modes may be present but not registered when using this measurement.

## 8 Experimental velocity profile of the plate surface

Torsional modes can be visualized as rotations about an axis of symmetry along the length of the plate. Measurements taken at any point on the axis will not register this type of mode. In [31] the importance of excitation configuration is illustrated for identifying all relevant modes. Here similar care is required when selecting the method of measuring output.

Taking kinematic measurements at a corner of the plate makes all out-of-plane modes observable. In subsequent experiments and simulations, resonances are identified using this method. Preliminary tests (Fig. 9) indicate additional modes to those observed using blocked force are present. Even after identification these modes cannot be characterised for validation using just a single measurement.

## 9 Method for combination of mobility frequency response measurements

Comparison of velocity profiles allows a comprehensive validation of the computational model with the experimental component. A composite of multiple point-wise velocity measurements is required in order to generate a 3-Dimensional (3D) representation of the frequency response

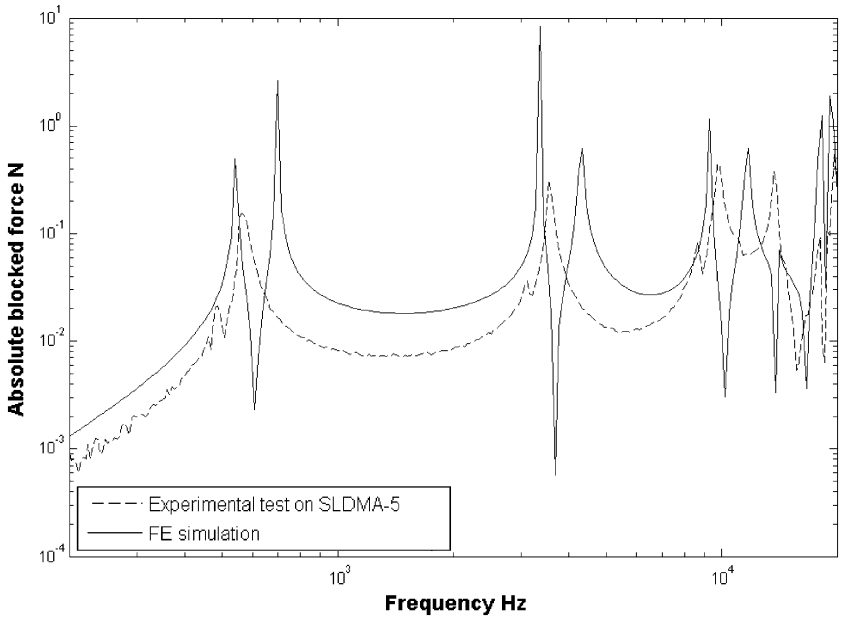


**Fig. 7** A comparison of the blocked force frequency response of an experimental SLDMA and the FE simulation. Experimental peaks appear to precede equivalent resonances in the modelled device

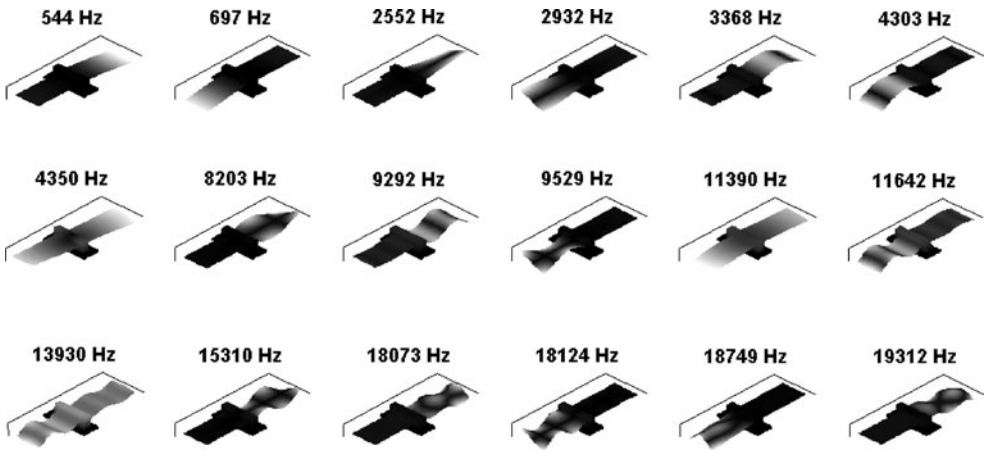


**Fig. 8** All 18 eigenmodes that exist in the audible frequency range of the FE SLDMA model

of the SLDMA. These measurements are mapped over the plate in a regular grid with a spacing of 1 mm in both axes. The whole of the laser vibrometer's measuring spot must be focused on the measured surface and so the grid of points used is 33 mm by 7 mm. The laser vibrometer is mounted on, and positioned with, two linear translation stages (Newport model 443-4) to ±10 μm. The data collected is converted to a grid of 231 velocity magnitudes and phases at a single frequency. Using a method outlined in [24] the operating velocity profile of the plate at each frequency is established.

For the method of approximating operating velocity profiles to be valid it is assumed that complex modes are not present. Even with non-proportional damping, caused by the epoxy layer and the joint between plate and stub, the resulting complexity can be assumed small. Other contributory factors would be modes located too closely and repeated roots. Using a 'peak-picking' method modal damping for the closest modes is of the order of less than 5%. The separation of the modes with this level of damping is 15-20%, sufficient to rule out complex modes. The FE stub offset and eigenmode analysis rule out any roots sharing a common frequency.

The absolute phase angle ($\varphi_a$), between the input voltage and output velocity, varied across the measured frequency range. At each frequency the phase angle ($\varphi_r$) is measured relative to the absolute phase at one of the corner of the measurement grid ($\varphi_c$) (3).

$$\varphi_r = \varphi_c - \varphi_a \tag{3}$$

The relative phase angle for a given frequency is consistently close to 0° or 180°. The only exceptions to this occur close to the stub and where velocities are small and merge with signal noise. Using the signum function of

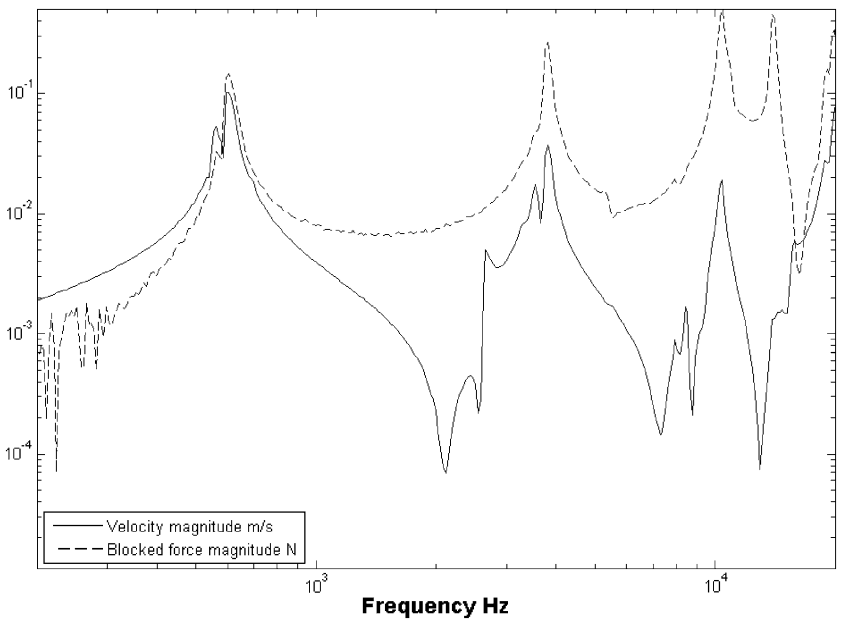


**Fig. 9** Additional modes demonstrated when measuring corner velocity, compared to those identifiable from the blocked force frequency response of SLDMA-3

cos($\varphi_r$) a positive or negative sign is applied to the velocity amplitudes ($v_A$ m/s) for each measurement (4).

$$v_m = v_A \mathrm{sgn}(\cos(\varphi_r)) \tag{4}$$

Mode shapes are generated by plotting the modal velocity ($v_m$) at each point on the grid of measurements for a given frequency. Linear interpolation is used between neighbouring points.

## 10 3D frequency response of the plate surface

To effectively validate the FE model it is necessary to compare the frequency response of the experimental SLDMA and confirm good agreement between them. The key characteristics to be matched are the resonant frequencies and operating velocity profiles at resonance. Only by characterising velocity profiles in 3D can resonances in the experimental environment be confidently compared with equivalent resonances in the FE model.

The development of operating mode shapes shown in Fig. 10 is comparable with the FE eigenmode analysis and the assumption of behavior analogous to cantilevered plates. The first pair has a similar profile to the static deflection of a cantilever under a uniformly distributed load. Between these there is a rocking mode at 494 Hz that illustrates a resonant peak in velocity contributing negligible blocked force.

As the frequency increases, resonances show an incremental addition of half sine waves on each side of the stub. The first half waves are shown at 3 kHz and 3.7 kHz, then at 8.7 kHz and 9.9 kHz and at 18.5 kHz and 19.7 kHz. The side of the stub that is not resonating also has a larger amplitude than shown in the eigenmode analysis.

The velocity frequency response at the corner of the plate shows the presence of two further modes without a peak in the blocked force response (2.6 kHz and 8.2 kHz). Both modes show a torsional vibration superimposed on the prevalent velocity profile along the plate length. This further confirms FE eigenmodes in the physical SLDMA. The appearance of the torsional modes is attributable to small asymmetries in the positioning of the piezoelectric layers on the brass plate across its width. In [2] the influence of PZT orientation is highlighted and although the manufacturing error is small in the SLDMA it is significant enough to actuate these modes.

The mode occurring at 15 kHz across the plate width is not suggested by the eigenmode analysis until higher frequencies. The presence of torsional modes and significant deformation in the width illustrates the importance of measuring and characterising response as a 3D plate rather than a 2D beam.

## 11 Comparison of experimental and FE velocity profiles

A frequency response analysis using the velocity profile of the whole surface was carried out on the FE model for comparison with experimental results. Figures 10 & 11

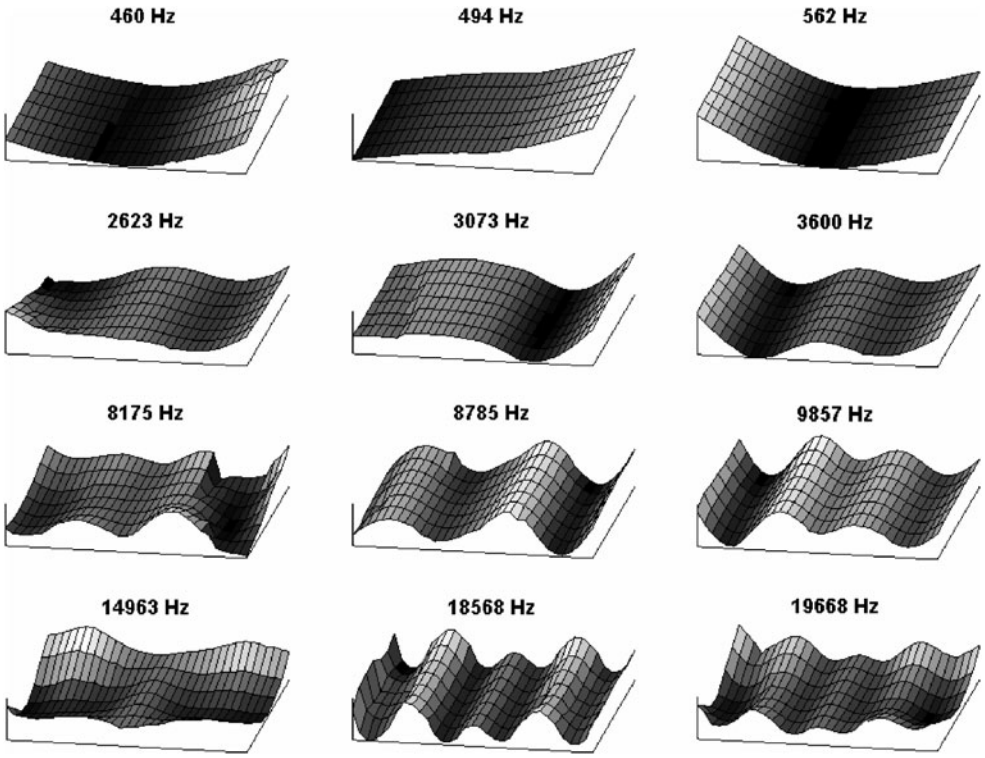


**Fig. 10** Profiles of the 12 identified resonances of SLDMA-5 showing modal progression, presence of torsional modes and the development of bending across the plate's width

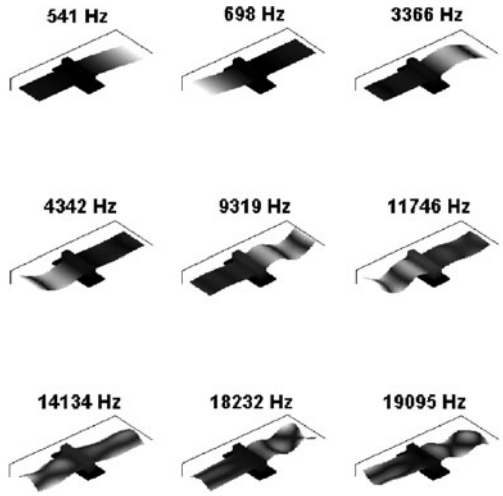


**Fig. 11** 3D velocity profiles obtained at corner resonances from the simulated SLDMA. Idealized symmetry prevents torsional modes from being excited. Results allow equivalent modes in the experimental device to be correlated

provide this comparison. The simulation results are more clearly defined than the experimental results due to its more refined mesh, higher order interpolation algorithms and idealised construction.

The FE velocity profiles match all important characteristics of the experiment at resonances identified at the corner of the plate. Good agreement is found in the shape and pairing of the modes. As frequency increases the FE simulation also shows the addition of sinusoidal half-waves to the profile first on the long side then on the short side of the stub.

The point in the sequence of modes where a half-wave profile is introduced into the width of the plate agrees with experiment. This takes place between operating modes with 1 and 1.5 sine waves along the plate lengths. Again this phenomenon is observable at a lower frequency than the eigenmodes of Fig. 8 suggest. The rocking mode highlighted at 494 Hz experimentally is also not a feature indicated by the eigenmode analysis. However the FE frequency response does demonstrate a similar profile between the first two bending modes.

The area where there is lack of agreement with the physical experiment is the presence of torsional modes. These are not excited in the simulation. This is due to the idealized symmetry in the width of the FE device rather than a failure in the modeling process. Evidence for this is the torsional eigenmodes that are present in the FE model.

With the level of confirmation provided by surface velocity profiles it is possible to identify the frequencies and sequence of equivalent operating modes necessary for validating the FE model. The FE response is shown to be consistent with experiment. The exceptions are at the highest two frequencies due to imperfect joints in the experimental component, a lack of clarity caused by residual effects of other modes in the physical experiment and material parameter approximations in the FE model. The latter would be improved in a full model updating procedure.

The merits of an updating exercise, using MAC for example, are limited in this case. A fully updated model would only correlate ideally with a single SLDMA in a set that shows significant variability and some uncertainty in model parameters. The aim of this investigation to validate the ability of FE software to model the current SLDMA devices and others of a similar type with limited variation in parameters has been achieved.

## 12 Conclusions

A general method for validation of a device too small for conventional modal analysis excitation has been demonstrated without the need for a scanning vibrometer. Initial discrepancies existing between the number of visible simulated FE and experimental modes are overcome. Operating blocked force in 1D and 2D velocity measurements are shown insufficient to characterise the SLDMA. Eigenmode analysis indicates the source of discrepancies and highlights the multi-dimensional response. Geometry of the device coupled with the self-actuation method requires validation to be carried out in 3D. Only then is the model considered validated and suitable for subsequent FE experimentation on minor modifications to material and geometric properties. These lessons learned will be universally applicable to the modelling of piezoelectric devices.

**Acknowledgements** This work was supported by EPSRC grants #GR/S63502/01 at the London School of Economics and #GR/S63496/02 at Brunel University. The authors thank NXT Sound for provision of the SLDMA devices and technical advice.

## References

1. R.J. Wood, E. Steltz, R.S. Fearing, Sensor. Actuat. A-Phys. **119**, 476–88 (2005)
2. R. Wetherhold, M. Messer, A. Patra, J. Eng, Mater-T. ASME. **125**, 148–52 (2003)
3. W. Zhang, G. Meng, H. Li, Int. J. Adv. Manuf. Technol. **28**, 321–7 (2006)
4. A. Preumont, *Mechatronics Dynamics of Electromechanical and Piezoelectric Systems* (Springer, Dordrecht, 2006)
5. K. Jian, M.I. Friswell, Mech. Syst. Signal Pr. **20**, 2290–2304 (2006)
6. V. Mortet, K. Haenen, J. Posmesil, M. Vanecek, M. D'Olieslaeger, Phys. Stat. Sol. **203**, 3185–90 (2006)
7. J.-C. Lin, M.H. Nien, Compos. Struc. **70**, 170–6 (2005)
8. H.F. Tiersten, *Linear Piezoelectric Plate Vibrations: Elements of the Linear Theory of Piezoelectricity & the Vibrations of Piezoelectric Plates* (Plenum, New York, 1969)

9. W.-Q. Chen, R.-Q. Xu, H.-J. Ding, J. Sound Vib. **218**, 741–8 (1998)
10. P. Cupial, J. Sound Vib. **283**, 1093–113 (2005)
11. A. Benjeddou, J.-F. Deü, Int. J. Solids Struct. **39**, 1463–86 (2002)
12. D.J. Gorman, J. Sound Vib. **49**, 453–67 (1976)
13. A.W. Leissa, J. Sound Vib. **31**, 257–93 (1973)
14. R.D. Blevins, *Formulas for Natural Frequency and Mode Shape* (Van Nostrand Reinhold, New York, 1979). ch.11
15. M.I. Friswell, J. Sound Vib. **241**, 361–72 (2001)
16. H. Allik, T.J. Hughes, Int. J. Numer. Meth. Eng. **2**, 151–7 (1970)
17. C.M. Mota-Soares, C.A. Mota-Soares, V.M. Franco Correia, Compos. Struct. **47**, 625–34 (1999)
18. A.C. Hladky-Hennion et al., J. Electroceram. **19**, 395–398 (2007)
19. K.-J. Lim, S.-H. Kang, J.-S. Lee, J. Electroceram. **13**, 429–432 (2004)
20. P. Vasiljev, S. Borodinas, L. Vasiljeva, D. Mazeika, S.-J. Yoon, J. Electroceram. **20**, 271–276 (2008)
21. S.D. Senturia, Sensor. Actuator. **67**, 1–7 (1988)
22. S.-Y. Lee, B. Ko, W. Yang, Smart Mater. Struct. **14**, 1343–52 (2005)
23. Z.K. Kusculuoglu, B. Fallahi, T.J. Royston, P. Soc, Photo-Opt. Inst. **4693**, 92–103 (2002)
24. D.J. Ewins, *Modal Testing Theory, Practice and Application* (Research Studies, Baldock, 2000)
25. R. Schnitzer, N. Rümmler, B. Michel, P. Soc, Photo-Opt. Inst. **3825**, 72–9 (2002)
26. X. Chu, L. Ma, S. Yuan, M. Li, L. Li, J. Electroceram. available online 2007
27. S.-M. Swei, P. Gao, R. Lin, Smart. Mater. Struct. **10**, 409–13 (2001)
28. J.S. Burdess, A.J. Harris, D. Wood, R.J. Pitcher, D. Glennie, J. Microelectromech. S. **6**, 322–8 (1997)
29. W.-P. Lai, W. Fang, Sensor. Actuator. **96**, 43–52 (2002)
30. O. Burak-Ozdoganlar, B.D. Hansche, T.G. Carne, Exp. Mech. **45**, 498–506 (2005)
31. M. Hu, J. Xie, S.-F. Ling, H. Du, Y. Fu, P. Soc, Photo-Opt. Inst. **5852**, 633–8 (2005)
32. A. Erturk, D.J. Inman, Smart Mater. Struct. **17**, art. no. 065016 (2008)
33. MatWeb Material Property Data. http://www.matweb.com. Accessed 2007
34. IEEE Standard on Magnetostrictive Materials: Piezomagnetic Nomenclature, IEEE Standard 319 (1990)
35. D.J. Gorman, *Free Vibration Analysis of Rectangular Plates* (Elsevier North Holland, New York, 1982)